

Absorption and Fluorescence of 2,5-Diarylidencyclopentanones in Acidic Media: Evidence for Excited-State Proton Transfer

Mine G. Ucak-Astarlioglu[†] and Robert E. Connors^{*}

Department of Chemistry and Biochemistry, Worcester Polytechnic Institute, Worcester, Massachusetts 01609

Received: June 1, 2005; In Final Form: July 26, 2005

Spectroscopic properties for a series of 2,5-diarylidencyclopentanones in weak and strong acid environments are reported. Electronic absorption and fluorescence spectra have been measured for the all-*E* configurations of 2,5-dibenzylidencyclopentanone (**1**), 2,5-bis(3-phenylallylidene)cyclopentanone (**2**), and 2,5-bis(5-phenylpenta-2,4-dienylidene)cyclopentanone (**3**) in acetic acid and sulfuric acid solutions. The spectroscopic evidence indicates that in 96% sulfuric acid **1**, **2**, and **3** are protonated both in the ground state and on the S_1 potential energy surface. This assignment is supported by Zerner's intermediate neglect of differential overlap (ZINDO) and time-dependent density functional theory (TD-DFT) calculations. In glacial acetic acid, **1**, **2**, and **3** are unprotonated in the ground state. The absence of observable fluorescence from **1** in glacial acetic acid indicates that S_1 is $n\pi^*$, whereas the observation of fluorescence from **2** and **3** in acetic acid is consistent with S_1 being $\pi\pi^*$. A combination of spectroscopic data, molecular orbital calculations, and fluorescence lifetime measurements indicate that **2** and **3** undergo intermolecular excited-state proton transfer in glacial acetic acid and diluted sulfuric acid solutions. Photochemical studies reveal that, unlike its behavior in organic solvents, **1** does not undergo efficient *E,E* \rightarrow *E,Z* photoisomerization in 96% sulfuric acid.

Introduction

In a recent publication we reported on the spectroscopic and photophysical properties of a series of 2,5-diarylidencyclopentanones in a number of organic solvents.¹ These diarylpolyene ketones and their substituted derivatives have received recent attention for potential applications in a variety of areas that take advantage of their photoexcited-state properties.^{2–16} In this work we extend our earlier study to a computational and spectroscopic investigation of these compounds and their protonated cations in acidic environments. Specifically, electronic absorption and fluorescence spectra have been measured for the all-*E* configurations of 2,5-dibenzylidencyclopentanone (**1**), 2,5-bis(3-phenylallylidene)cyclopentanone (**2**), and 2,5-bis(5-phenylpenta-2,4-dienylidene)cyclopentanone (**3**) in acetic acid and sulfuric acid solutions of various strengths. Density functional theory (DFT), time-dependent density functional theory (TD-DFT), and Zerner's intermediate neglect of differential overlap (ZINDO) calculations have been carried out for the oxygen-protonated cations of these compounds (see Figure 1), which will be designated $1H^+$, $2H^+$, and $3H^+$, respectively. Spectroscopic, molecular modeling and fluorescence lifetime data indicate that **2** and **3** undergo intermolecular excited-state proton transfer in glacial acetic acid and diluted sulfuric acid. A brief photochemical study of **1** and $1H^+$ has been performed and analyzed by HPLC to determine if *E,E* \rightarrow *E,Z* photoisomerization takes place in sulfuric acid solution as it has been shown to in organic solvents.¹⁷

Experimental Section

The spectroscopic facilities and the preparation of 2,5-diarylidencyclopentanones used in this study have been

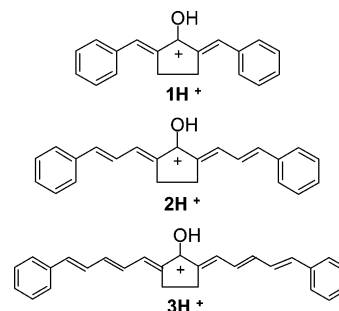


Figure 1. Structures of protonated 2,5-diarylidencyclopentanones $1H^+$, $2H^+$, and $3H^+$.

described previously.¹ Glacial acetic acid and sulfuric acid (ACS grade) were found to be free of absorbing and emitting impurities and used as received. It was observed that **3** undergoes unknown reaction(s) beyond oxygen protonation in 96% sulfuric acid. Solutions of **3** in a 1:3 mixture of 96% sulfuric acid and acetic acid appear to be free of the side reactions. This mixture was used for **3** only in place of 96% sulfuric acid and for simplicity is referred to as 96% sulfuric acid in the text. Fluorescence lifetimes were measured by M.G.U. in the laboratory of M. Maroncelli at the Pennsylvania State University, University Park, PA. Photochemical irradiations were performed with a 150 W xenon arc lamp filtered through 15 cm of distilled water. Irradiated solutions of $1H^+$ in sulfuric acid were neutralized with aqueous $NaHCO_3$, extracted with ethyl ether, dried over $MgSO_4$, and analyzed by HPLC. Molecular modeling was performed with Gaussian 03 software.¹⁸ ZINDO calculations¹⁹ employing complete sets of singly excited configurations (CIS) were carried out by use of the default parameters within Gaussian 03.

^{*} Corresponding author: e-mail rconnors@wpi.edu.

[†] Present address: Department of Chemistry, The Pennsylvania State University, University Park, PA 16802.

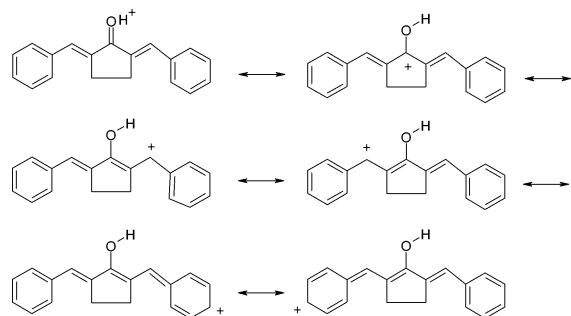


Figure 2. Resonance structures for 1H^+ .

TABLE 1: Bond Lengths and Bond Orders Calculated by B3LYP/6-31G(d) for **1** and 1H^+

parameter	bond length (Å)		bond order	
	1	1H^+	1	1H^+
OH		0.973		0.71
CO	1.226	1.325	1.70	1.15
C=C	1.351	1.379	1.70	1.54
C-phenyl	1.460	1.441	1.12	1.20

Results and Discussion

Optimized Geometries and Spectral Calculations for Protonated Cations. Since it is anticipated that the oxygen protonated cations shown in Figure 1 will be present in highly acidic environments, computational studies of their molecular structures and electronic absorption spectra were performed. Agreement between computed and experimental spectra would lend support to the presence of the protonated cations in solution. The B3LYP/6-31G(d) optimized ground-state structures of 1H^+ , 2H^+ , and 3H^+ were found to have similar geometric parameters. Bond lengths are predicted to fall in the range 1.325–1.337 Å for C–O, 0.971–0.973 Å for O–H, and 1.436–1.447 Å for C–phenyl. In the cases of 2H^+ and 3H^+ , the remaining exocyclic C–C single bond lengths are computed to be in the range of 1.412–1.419 Å. The exocyclic double-bond lengths fall between 1.368 and 1.382 Å. Phenyl group rotations relative to the cyclopentanone ring are predicted to be $\sim 3^\circ$ out of plane for 1H^+ and 0.01° for 2H^+ and 3H^+ . The C–O–H bond angles are calculated to be 109.5° for 1H^+ , 109.2° for 2H^+ , and 109.0° for 3H^+ .

In Table 1 a comparison of bond lengths and bond orders for **1** and 1H^+ is made. In addition to the expected difference in CO bond length, it is observed that the exocyclic double bond shows an increase in bond length and a decrease in bond order in going from the neutral to protonated form, whereas a change in the opposite direction is observed for the single bond connected to the phenyl group. It is appealing to suggest that the differences in bond lengths and bond orders between **1** and 1H^+ indicate that the resonance forms shown on the second and third lines of Figure 2 make a greater contribution to the electronic structure of 1H^+ than do analogous resonance structures for **1**.

The optimized geometries of 1H^+ , 2H^+ , and 3H^+ were used as input for TD-DFT (B3LYP/6-31G(d)) and ZINDO–CIS spectral calculations. Room-temperature absorption spectra of protonated **1**, **2**, and **3** dissolved in 96% sulfuric acid are shown in Figure 3 along with the results of the ZINDO calculations. TD-DFT yielded similar computational results; however, ZINDO exhibited somewhat better overall agreement with experiment. Only the $S_0 \rightarrow S_1$ transition computed by TD-DFT is presented in Figure 3. Agreement between the ZINDO-computed spectra of 1H^+ , 2H^+ , and 3H^+ and the experimental spectra in

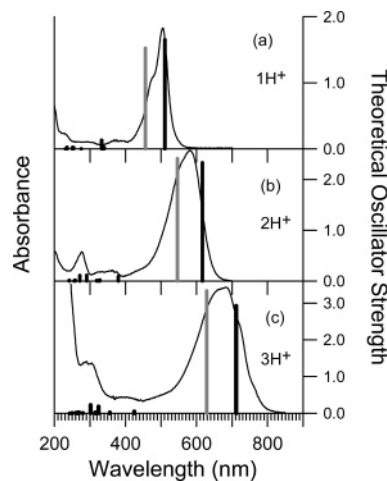


Figure 3. Room-temperature absorption spectra in 96% sulfuric acid and ZINDO calculated results (black bars): (a) 1H^+ , (b) 2H^+ , and (c) 3H^+ . The gray bars represent the $S_0 \rightarrow S_1$ transition computed by TD-DFT.

sulfuric acid is excellent. The TD-DFT and ZINDO calculations agree that the $S_0 \rightarrow S_1$ transition arises primarily from the highest occupied molecular orbital (HOMO) \rightarrow lowest unoccupied molecular orbital (LUMO) excitation and is $\pi \rightarrow \pi^*$ in nature for the three protonated cations (1H^+ , 2H^+ , and 3H^+). This transition correlates with $S_0 \rightarrow S_2$ computed by ZINDO for the unprotonated forms (**1**, **2**, and **3**), while $S_0 \rightarrow S_1$ was found to be $n \rightarrow \pi^*$ for unprotonated **1**, **2**, and **3**.¹ A red shift of 1.1–1.2 eV for the lowest energy $\pi \rightarrow \pi^*$ excitation upon going from hydrocarbon solvent¹ to sulfuric acid is consistent with a change from neutral (**1**, **2**, and **3**) to oxygen-protonated forms (1H^+ , 2H^+ , and 3H^+). Shifts of this magnitude between neutral and oxygen-protonated α,β -unsaturated aldehydes and ketones in the gas phase have been reported.²⁰ Thus the spectral calculations and experimental data support formation of oxygen-protonated cations in 96% sulfuric acid.

Acetic Acid. It was found that **2** and **3**, but not **1**, fluoresce in glacial acetic acid. The room-temperature absorption, fluorescence, and fluorescence excitation spectra of **2** and **3** in glacial acetic acid and acetic acid- d_1 are presented in Figure 4. For each compound the fluorescence spectrum consists of two overlapping bands (535 and 615 nm for **2** in acetic acid; 606 and 685 nm for **3** in acetic acid). The excitation spectrum of each compound does not change when the monitoring wavelength is moved from the shorter wavelength fluorescence band to the longer wavelength band. Fluorescence lifetimes were measured for **2** in acetic acid at approximately 40 nm intervals between 550 and 650 nm and fits to one, two, and three exponential decays were explored. The best fit of the data is found to be two exponentials with lifetimes of 33 and 85 ps. The amplitude of the faster decay decreases with increasing fluorescence wavelength, whereas that of the slower decay increases.

The effect of dilution with water on the spectroscopic properties of **2** in acetic acid was explored. Spectra corresponding to **2** in acetic acid diluted with water to approximately pH = 2.5 are shown in Figure 5. In comparing Figures 4a and 5, it is observed that the relative intensity of the fluorescence band at 615 nm decreases when the glacial acetic acid solution is diluted to pH = 2.5. Further dilution with water causes this band to disappear completely. The lack of complete overlap of the absorption and excitation spectra in glacial acetic acid suggests that under these conditions more than one species exists in solution, for example, strongly hydrogen-bonded and weakly

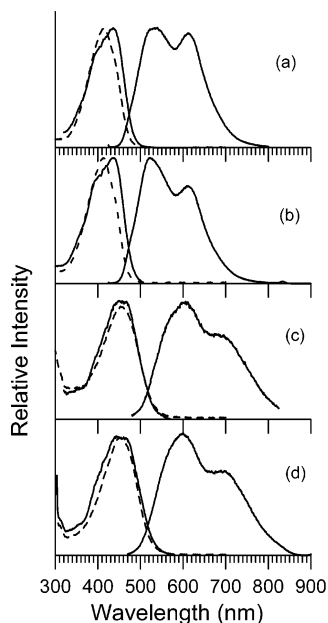


Figure 4. Normalized absorption (dashed line), excitation (left), and fluorescence (right) spectra: (a) **2** in glacial acetic acid; (b) **2** in acetic acid- d_1 ; (c) **3** in glacial acetic acid; and (d) **3** in acetic acid- d_1 .

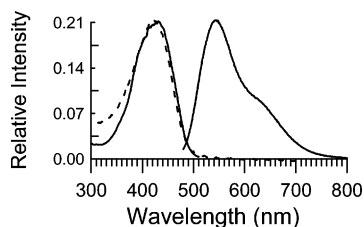


Figure 5. Normalized absorption (dashed line), excitation (left), and fluorescence (right) spectra of **2** in acetic acid solution (pH = 2.5).

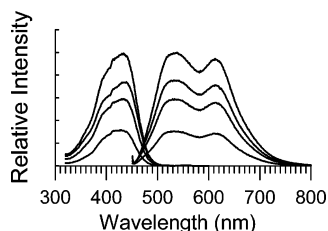


Figure 6. Excitation (left) and fluorescence (right) spectra of **2** at various concentrations in glacial acetic acid.

hydrogen-bonded forms of **2**. At the higher pH of 2.5, better overlap of the absorption and excitation spectra suggests a more homogeneous solution. Similar lack of complete spectral overlap has been observed for **2** in alcoholic solvents.¹

To eliminate the possibility that the longer wavelength band observed in the fluorescence spectra of **2** in acetic acid is due to ground-state aggregation or excited-state excimer formation, a concentration study of **2** in acetic acid was conducted and is shown in Figure 6. A stock solution of the compound was prepared in glacial acetic acid and spectra were recorded at various concentrations by taking an aliquot of the stock solution and adding more glacial acetic acid. If aggregation/excimer effects were contributing to the long-wavelength band, the band should diminish in intensity relative to the shorter wavelength band upon dilution by the addition of glacial acetic acid. It is observed that the intensities of the two bands remain constant relative to each other, thus eliminating aggregation/excimer formation as an explanation for the observed spectral features.

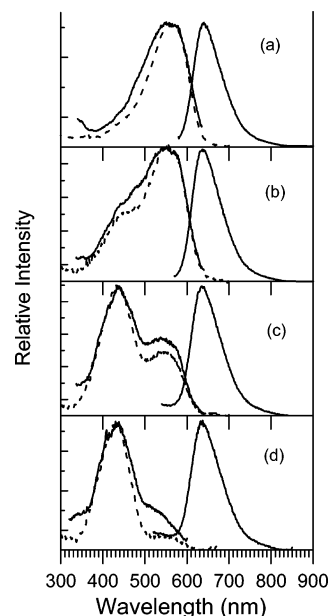


Figure 7. Normalized absorption (dashed line), excitation (left), and fluorescence (right) spectra of **2** in sulfuric acid solutions: (a) 96%; (b) pH = 1.0; (c) pH = 1.4; and (d) pH = 1.6.

Sulfuric Acid. Figure 7 presents absorption and fluorescence data for **2** dissolved in (a) 96% sulfuric acid and in sulfuric acid solutions diluted with water having pH values approximately equal to (b) 1.0, (c) 1.4, and (d) 1.6. In 96% sulfuric acid, broad absorption and fluorescence bands are observed for **2** at 570 and 630 nm, respectively. Upon dilution with water, a new absorption band is seen to grow in at approximately 440 nm while the absorption at 570 nm decreases in relative intensity. The fluorescence band at 630 nm remains relatively unchanged in appearance for the range of dilutions (pH) studied. Fluorescence excitation spectra are in reasonable agreement with the absorption spectra over the range of pH investigated.

Protonation. From the studies of **2** in acidic media, a fairly clear picture arises. In 96% sulfuric acid there is essentially complete protonation of the ketone, both in the ground state and in the excited state. As the sulfuric acid solution is diluted and the pH increases, the growth of the absorption band at 440 nm is attributed to absorption by ground-state unprotonated **2**. A ground-state equilibrium is established between protonated and unprotonated **2** that can be shifted from one form to the other by altering the pH. The fact that fluorescence is observed only at 630 nm for the range of sulfuric acid strengths studied indicates that in all cases emission is observed from protonated **2** only. The absence of fluorescence from unprotonated **2** in diluted sulfuric acid solutions where it is known to be present in significant amounts relative to protonated **2**, for example, pH = 1.4–1.6, indicates that under these conditions **2** undergoes a highly efficient excited-state proton-transfer reaction on the S_1 surface, forming the protonated cation prior to emission.

In glacial acetic acid the situation is somewhat different in that there is no evidence of ground-state protonation of **2** in the absorption spectra; however, the fluorescence spectrum presented in Figure 4a shows two bands with different lifetimes, consistent with emission from both unprotonated (535 nm) and protonated (615 nm) **2**. In this case protonation is occurring only on the excited-state surface, but to a lesser degree than for the sulfuric acid solutions discussed previously. As a result, emission from unprotonated and protonated excited-state species contribute to the fluorescence spectrum in glacial acetic acid.

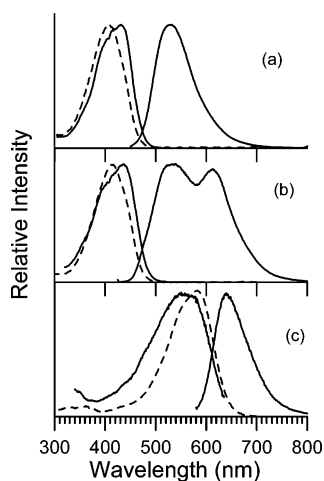


Figure 8. Normalized absorption (dashed line), excitation (left), and fluorescence (right) spectra of **2** in acidic media: (a) methanol; (b) glacial acetic acid; and (c) 96% sulfuric acid.

Increasing the pH of the acetic acid solution to 2.5, as shown in Figure 5, shifts the excited-state equilibrium toward unprotonated **2**.

From Figure 4c, it is seen that results similar to those found for **2** are observed for **3**. In acetic acid media a single absorption band is observed, whereas two emission bands exist. The similarity of these spectra to those of **2** in acetic acid suggests that excited-state proton transfer also takes place for **3** in this solvent. Experimental difficulties prevented measurement of fluorescence lifetimes for **3** in acetic acid.

Earlier work from our laboratory demonstrated that S_1 is a nonfluorescent $n\pi^*$ state for **1**, **2**, and **3** in nonpolar solvents.¹ A state inversion placing the fluorescent $\pi\pi^*$ (HOMO \rightarrow LUMO) state below the $n\pi^*$ state is observed in alcoholic solvents for **2** and **3** as well as in some polar solvents for **3**; however, **1** was nonfluorescent in all of the solvents studied, indicating that S_1 remained $n\pi^*$. The failure to observe fluorescence from **1** in acetic acid, including emission from $\mathbf{1H}^+$, suggests that S_1 is $n\pi^*$ in this solvent also. As with alcoholic solvents, S_1 is expected to be $\pi\pi^*$ for unprotonated **2** and **3** in acetic acid. The observation of excited-state proton transfer when S_1 is $\pi\pi^*$ but not when S_1 is $n\pi^*$ can be understood by considering that there is a transfer of electron charge density to the carbonyl oxygen upon excitation from S_0 to S_1 ($\pi\pi^*$), making the molecule a stronger base in the excited state, thus promoting excited-state proton transfer from a neighboring acid. Conversely, a reduction in electron charge density on the oxygen atom occurs when S_1 is $n\pi^*$, making the molecule a weaker base in the excited state. This interpretation is supported by ZINDO Mulliken population analyses, which have been carried out for **1** and show that the partial charge on oxygen changes from -0.53 in the ground state to -0.081 and -0.63 in the lowest energy $n\pi^*$ and $\pi\pi^*$ singlet states, respectively. Quantitative experimental results related to the change in base strength upon photoexcitation may be obtained for **2** and **3** from the fluorescence spectrum of each in glacial acetic acid. By using the two maxima appearing in the fluorescence spectrum as a measure of the energies of the unprotonated and protonated forms of the molecule in S_1 , the increase in pK_a of the conjugate acid may be determined by application of the Förster cycle.²¹ The $pK_a^* - pK_a$ values obtained in this approach are 5.2 for $\mathbf{2H}^+$ and 4.1 for $\mathbf{3H}^+$.

Figure 8 shows the room-temperature absorption, excitation, and fluorescence spectra of **2** in (a) methanol, (b) glacial acetic acid, and (c) 96% sulfuric acid solvents. As the acidity of the

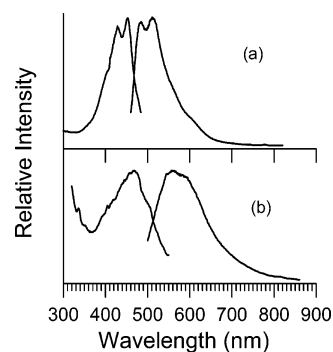


Figure 9. Fluorescence and fluorescence excitation spectra in glacial acetic acid at 77 K: (a) **2** and (b) **3**.

solvents increases, a progression is observed from absorption and emission of hydrogen-bonded but not protonated species (methanol), followed by absorption by hydrogen-bonded and emission from hydrogen-bonded and protonated molecules (glacial acetic acid), and finally to absorption and emission from protonated species (96% sulfuric acid). The same trend is observed for **3** in these three solvents.

Comparisons of the absorption and fluorescence properties in acetic acid and acetic acid- d_1 for **2** (Figure 6a,b) and **3** (Figure 6c,d) show that although the spectra are similar in the undeuterated and deuterated solvents, the ratio of unprotonated to protonated emission increases for **2** but is essentially unchanged for **3** when these molecules are placed in acetic acid- d_1 . These results suggest that **2** and **3** in various acidic solvents may be interesting systems for testing the various theories that have been proposed to describe the kinetic, thermodynamic, and isotopic influences on excited-state proton transfer.²²

Finally, it is worth noting in this section that, when dissolved in tetrahydrofuran (THF)¹⁷ or methanol, **1** undergoes rapid $E,E \rightarrow E,Z$ photoisomerization about one of its exocyclic double bonds; whereas prolonged irradiation of $\mathbf{1H}^+$ in 96% sulfuric acid reveals no indication of $E,E \rightarrow E,Z$ photoconversion.

Low-Temperature Spectra. Low-temperature fluorescence and fluorescence excitation spectra have been measured for **1**, **2**, and **3** in acidic media. Figure 9 shows spectra at 77 K for **2** and **3** in glacial acetic acid. It is seen that some vibronic structure is resolved in the fluorescence and excitation spectra of **2**. The apparent 0–0 bands occur at 484 nm in fluorescence and 452 nm in the excitation spectrum. This is a blue shift from the fluorescence maximum of 535 nm and a red shift from the 484 nm excitation maximum observed at room temperature in this solvent. As a result, there is a considerably smaller Stokes' shift at low temperature. A shoulder in the fluorescence spectrum at 600–610 nm may be from the protonated cation, suggesting that the degree of excited-state protonation has been quenched considerably compared to room temperature. For **3** in glacial acetic acid, the shift from room temperature to low temperature follows a similar pattern, shifting from 606 to 560 nm in fluorescence and from 449 to 470 nm in the excitation spectrum. There is no indication of emission that can be assigned to the protonated cation. However, the spectrum is broad and a small amount of cation emission, if present, may not be resolvable.

Figure 10 presents the fluorescence and fluorescence excitation spectra of $\mathbf{1H}^+$, $\mathbf{2H}^+$, and $\mathbf{3H}^+$ in 96% sulfuric acid at 77 K. Resolved vibronic structure is observed for $\mathbf{1H}^+$ and $\mathbf{2H}^+$ with red shifts in fluorescence and blue shifts in absorption relative to room temperature for both species, resulting in small Stokes' shifts. In the case of $\mathbf{3H}^+$, the spectra remain broad at low temperature and the low temperature shifts are smaller. Small Stokes' shifts are commonly observed for molecules in

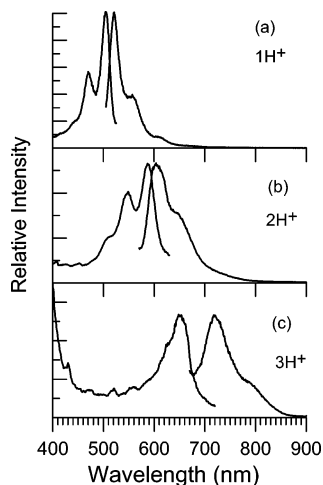


Figure 10. Fluorescence and fluorescence excitation spectra in 96% sulfuric acid at 77 K: (a) 1H^+ , (b) 2H^+ , and (c) 3H^+ .

low-temperature glasses and are attributed to the inability of the solvent matrix to reorient and stabilize the molecule during the excited-state lifetime. Attempts to observe phosphorescence out to 900 nm at 77 K for **1**, **2**, and **3** in acetic acid and in sulfuric acid were unsuccessful.

Conclusion

Evidence has been offered that shows that **2** and **3** undergo S_1 excited-state proton transfer in glacial acetic acid and diluted sulfuric acid solutions at room temperature. The luminescence properties are consistent with S_1 being $n\pi^*$ for **1** and $\pi\pi^*$ for **2** and **3** in glacial acetic acid. Examination of the computed charge on oxygen for **1** demonstrates that the lowest $\pi\pi^*$ state is a stronger base than the lowest $n\pi^*$ state. Absorption, fluorescence, and spectral calculations reveal that **1**, **2**, and **3** dissolved in 96% sulfuric acid are protonated in the ground state and on S_1 . Photochemical studies show that 1H^+ does not undergo $E,E \rightarrow E,Z$ photoisomerization under conditions that induce photoisomerization for **1**.

Acknowledgment. We thank M. Maroncelli and N. Ito for their assistance with the fluorescence lifetime measurements.

References and Notes

- (1) Connors, R. E.; Ucak-Astarlioglu, M. G. *J. Phys. Chem. A* **2003**, *107*, 7684.
- (2) Barnabus, M. V.; Liu, A.; Trifunac, A. D.; Krongauz, V. V.; Chang, C. T. *J. Phys. Chem.* **1992**, *96*, 212.
- (3) Chambers, W. J.; Eaton, D. F. *J. Imaging Sci.* **1986**, *30*, 230.
- (4) Baum, M. D.; Henry, C. P. U.S. Patent 3,652,275.
- (5) Pivovarenko, V. G.; Klueva, A. V.; Doroshenko, A. O.; Demchenko, A. P. *Chem. Phys. Lett.* **2000**, *325*, 389.
- (6) Das, P. K.; Pramanik, R.; Banerjee D.; Bagchi, S. *Spectrochim. Acta A* **2000**, *56*, 2763.
- (7) Doroshenko, A. O.; Grigorovich, A. V.; Posokhov, E. A.; Pivovarenko, V. G.; Demchenko, A. P. *Mol. Eng.* **1999**, *8*, 199.
- (8) Kawamata, J.; Inoue, K.; Inabe, T. *Bull. Chem. Soc. Jpn.* **1998**, *71*, 2777.
- (9) Kawamata, J.; Inoue, K.; Inabe, T.; Kiguchi M.; Kato, M.; Taniguchi, Y. *Chem. Phys. Lett.* **1996**, *249*, 29.
- (10) Kaatz, P.; Shelton, D. P. *J. Chem. Phys.* **1996**, *105*, 3918.
- (11) Kawamata, J.; Inoue, K.; Inabe, T. *Appl. Phys. Lett.* **1995**, *66*, 3102.
- (12) Theocharis, C. R.; Alison, M. C.; Hopkin, S. E.; Jones, P.; Perryman, A. C.; Usanga, F. *Mol. Cryst. Liq. Cryst. Incorporating Nonlinear Opt.* **1988**, *156*, 85.
- (13) Frey, H.; Behmann, G.; Kaupp, G. *Chem. Ber.* **1987**, *120*, 387.
- (14) Theocharis, C. R.; Jones, W.; Thomas, J. M.; Montevalli, M.; Hursthouse, B. *J. Chem. Soc., Perkin Trans. 2* **1984**, 71.
- (15) Theocharis, C. R.; Thomas, J. M.; Jones, W. *Mol. Cryst. Liq. Cryst.* **1983**, *93*, 53.
- (16) Shannigrahi, M.; Bagchi, S. *J. Phys. Chem. B* **2004**, *108*, 17703.
- (17) George, H.; Roth, H. J. *Tetrahedron Lett.* **1971**, *43*, 4057.
- (18) (a) Frisch, M. J.; Trucks, G. W.; Schlegel, H. B.; Scuseria, G. E.; Robb, M. A.; Cheeseman, J. R.; Montgomery, J. A., Jr.; Vreven, T.; Kudin, K. N.; Burant, J. C.; Millam, J. M.; Iyengar, S. S.; Tomasi, J.; Barone, V.; Mennucci, B.; Cossi, M.; Scalmani, G.; Rega, N.; Petersson, G. A.; Nakatsuji, H.; Hada, M.; Ehara, M.; Toyota, K.; Fukuda, R.; Hasegawa, J.; Ishida, M.; Nakajima, T.; Honda, Y.; Kitao, O.; Nakai, H.; Klene, M.; Li, X.; Knox, J. E.; Hratchian, H. P.; Cross, J. B.; Adamo, C.; Jaramillo, J.; Gomperts, R.; Stratmann, R. E.; Yazyev, O.; Austin, A. J.; Cammi, R.; Pomelli, C.; Ochterski, J. W.; Ayala, P. Y.; Morokuma, K.; Voth, G. A.; Salvador, P.; Dannenberg, J. J.; Zakrzewski, V. G.; Dapprich, S.; Daniels, A. D.; Strain, M. C.; Farkas, O.; Malick, D. K.; Rabuck, A. D.; Raghavachari, K.; Foresman, J. B.; Ortiz, J. V.; Cui, Q.; Baboul, A. G.; Clifford, S.; Cioslowski, J.; Stefanov, B. B.; Liu, G.; Liashenko, A.; Piskorz, P.; Komaromi, I.; Martin, R. L.; Fox, D. J.; Keith, T.; Al-Laham, M. A.; Peng, C. Y.; Nanayakkara, A.; Challacombe, M.; Gill, P. M. W.; Johnson, B. G.; Chen, W.; Wong, M. W.; Gonzalez, C.; Pople, J. A. *Gaussian 03*, Revision B.04; Gaussian, Inc.: Pittsburgh, PA, 2003. (b) Stratmann, R. E.; Scuseria, G. E.; Frisch, M. E. *J. Chem. Phys.* **1998**, *109*, 8218.
- (19) Ridley, J.; Zerner, M. *Theor. Chim. Acta* **1973**, *32*, 111.
- (20) Honovich, J. P.; Dunbar, R. C. *J. Phys. Chem.* **1981**, *85*, 1558.
- (21) (a) Förster, Th. *Naturwissenschaften* **1949**, *36*, 186. (b) Förster, Th. *Z. Electrochem.* **1950**, *54*, 531.
- (22) Tolbert, L. M.; Solntsev, K. M. *Acc. Chem. Res.* **2002**, *35*, 19.